Microsyst Technol (2011) 17:429–436
DOI 10.1007/s00542-011-1252-8

TECHNICAL PAPER

Auto-calibration of capacitive MEMS accelerometers based on pull-in voltage

L. A. Rocha · R. A. Dias · E. Cretu · L. Mol · R. F. Wolffenbuttel

Received: 17 November 2010 / Accepted: 2 February 2011 / Published online: 18 February 2011

Abstract This paper describes an electro-mechanical auto-calibration technique for use in capacitive MEMS accelerometers. Auto-calibration is achieved using the combined information derived from an initial measurement of the resonance frequency and the measurement of the pull-in voltages during device operation, with an estimation of process-induced variations in device dimensions from layout and deviations in material properties from the known nominal value. An experiment-based analytical model is used to compute the required electrostatic forces required to simulate external accelerations allowing the electro-mechanical calibration of the accelerometer. Measurements on fabricated devices confirm the validity of the proposed technique and electro-mechanical calibration is experimentally demonstrated.

1 Introduction

MEMS technologies have made enormous progress and are presently at a level of maturity that is comparable to that of technologies available for integration of analogue or digital circuits. As a consequence high performance MEMS devices have become available, which have found widespread application. However, there are two notable deficiencies; design tools and testing and calibration capabilities. Much research has been carried out on the development of design tools aiming on an accurate prediction of the static and dynamic performance of MEMS devices, which is more complex as compared to tools for micro-electronic circuits design, because of the fact that MEMS devices generally operate in several domains simultaneously (e.g. electrical, mechanical and fluidic). Such tools have become available and greatly add to the commercial success and impact of MEMS (Senturia 2003). Relatively little attention is being paid to testing and auto-calibration issues. Design for testability is standard in circuit design and built-in-self-test (BIST) systems are standard parts in complex CMOS systems (Wang et al. 2006). There are several reasons for the reluctant introduction of testing and auto-calibration in MEMS, despite the obvious benefits:

– research on MEMS devices has mainly focused on technology, design and packaging with little work on test and calibration,
– testing of MEMS devices is not a trivial task: MEMS devices involve multiple energy domains and therefore the large amount of failure mechanisms require, in many cases, complex models.

Testing/calibration of MEMS devices could have huge impact at both the economical and operational aspects; economically, because the packaging cost in MEMS devices is high and it is therefore important to identify a failure in the structure as soon as possible (i.e. wafer level testing rather than die testing, which in turn is preferred to testing after assembly in a system-in-a-package). Validation of proper operation of the device is as important,

L. A. Rocha (✉) · R. A. Dias
School of Engineering, University of Minho,
Campus de Azurem, 4800-058 Guimaraes, Portugal
e-mail: lrocha@dei.uminho.pt

E. Cretu
Department of Electrical and Computer Engineering,
University of British Columbia, 2332 Main Mall,
Vancouver, BC V6T 1Z4, Canada

L. Mol · R. F. Wolffenbuttel
Faculty EEMCS, Department for Microelectronics,
Delft University of Technology, Mekelweg 4,
2628 CD Delft, The Netherlands

especially in case failure may lead to a dangerous situation (e.g. airbags). Even if the importance of testing is recognized, a successful testing system should be fast, low-cost, and occupy a very small size, if it is going to be adopted in a high-volume manufacturing environment.

The first attempts to include a simple testing mechanism in accelerometer operation date back to the end of the 1980s and involve the electrostatic actuation to deflect the proof mass and provide self testing capabilities (Allen et al. 1989). Since then a few other methodologies, following similar approaches, have been proposed for accelerometer testing (Charlot et al. 2001; Mir et al. 2006; Olbrich et al. 1997; Puers and Reyntjens 2002; Xiong et al. 2005). The test is limited to the verification whether the mass is free to move and an electrical signal is used to stimulate the device. Based on the response we can have a PASS/FAIL scenario, where the devices not responding to the stimulus are rejected. This self-test is widely used in commercial accelerometers in the automotive application (Analog Devices 2010). It offers a simple test mechanism to access the accelerometer functional state (confidence on the device functionality), which is crucial for user acceptance of an airbag system.

It is generally not possible to extend the self-test to a technique that can quantitatively calibrate the accelerometer. In theory several pre-defined voltages can be applied to generate electrostatic forces that can be used to simulate several equivalent accelerations, which can be used to calibrate the system. However, too many tolerances prevent a straightforward implementation of such a principle. Calibration of a commercially available accelerometer at several accelerations in the operating range and at several temperatures is usually mandatory and this makes it the most expensive part of accelerometer manufacturing. Basic accelerometer calibration (as an example we consider a ± 1 g accelerometer) is usually done by applying first a 1 g test acceleration signal, followed by a test acceleration of -1 g (e.g. by aligning the sensitivity axis along the earth gravity field) and checking the response of the sensor in the two cases. Auto-calibration capabilities have therefore the potential to introduce a substantial advantage: autonomous self-calibrated inertial sensors.

This paper presents an electro-mechanical calibration technique for capacitive MEMS accelerometers based on the measurement of pull-in voltages. Pull-in (Rocha et al. 2004) is a unique feature of gap-varying capacitive MEMS devices, and can provide detailed information about their characteristics. Since the attractive force due to an electrostatic field is inversely proportional to the square of the deflection, while the restoring elastic force is (to a first approximation) linear with deflection, an unstable system results in case of a deflection, δ, beyond a critical value, δ_{crit}. The pull-in voltage, V_{pi}, is defined as the voltage that is required to obtain this critical deflection and depends mainly on geometry, residual stress level and material properties. Pull-in causes the displacement range due to electrostatic force to be limited to 1/3 of the gap between the electrodes, in case of a gap-varying motion of the movable capacitor plate. Pull-in based test structures are used, among other applications, for characterizing structural materials in surface micromachining processes (Cho et al. 1992; Osterberg and Senturia 1997).

The new concept for auto-calibration introduced here results from previous work on process characterization based on pull-in voltage measurement techniques (Rocha et al. 2004, 2008). In fact, when pull-in voltage measurements are combined with the measurement of the resonance frequency (a single measurement is needed), fabrication process non-idealities, such as over-etching and process asymmetries, can be accurately estimated. The models extracted from the measurements provide an equivalent calibration capability (replacement of an external inertial force of ± 1 g) using electronic excitation only.

2 Background theory on the pull-in voltage (1DOF)

The analysis of the essential characteristics of the pull-in voltage for one-degree-of-freedom (1DOF) devices requires only a simple micromechanical system composed of three electrodes. Two of them have a fixed position on the rigid supporting substrate, while the middle one is movable and connected to an elastic suspension with the spring constant k (Fig. 1a). This is the standard (differential) configuration of sensing and actuation elements in a capacitive inertial sensor.

When a voltage is applied across one of the equivalent capacitors, the static balance between the elastic and electrostatic forces defines the new equilibrium position of the movable plate. Its stability is given by the rate of variations of the two forces for small perturbations around the equilibrium point, that is, by the second derivative of the global potential energy. For a stable equilibrium, the second derivative of the global potential energy of the system with respect to deflection should be positive: $\partial^2 U_p / \partial x^2 > 0$; thus the pull-in voltage (V_{pi}) results as the solution of the two equations corresponding to $\partial U_p / \partial x = 0$ (force equilibrium) and $\partial^2 U_p / \partial x^2 = 0$ (margin of stability). The value of the pull-in voltage is determined by the elastic flexure material and dimensions, residual stress, and the geometry of the electrodes.

The geometry of the structure allows the definition of two pull-in voltages, as shown in Fig. 1a: asymmetric-right (V_{pr}), and asymmetric-left (V_{pl}). They will be equal in ideal conditions (perfectly symmetric structure), as can be

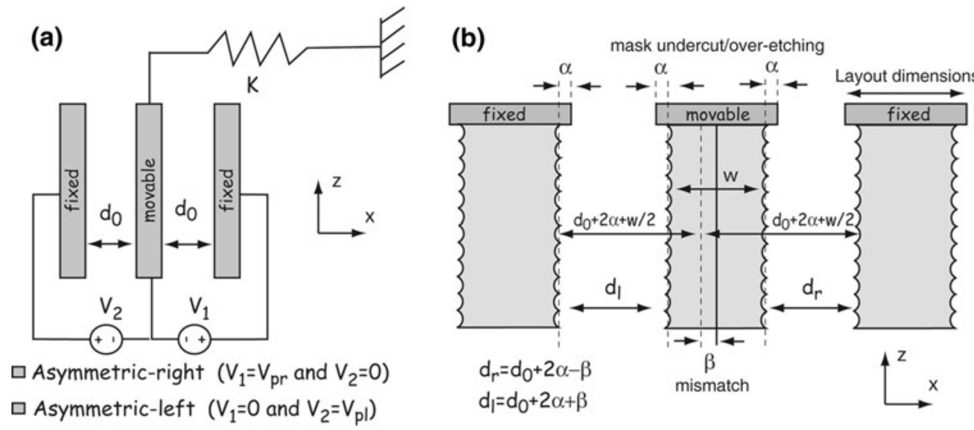

Fig. 1 Schematic of the basic electro-mechanical device with **a** ideal processing conditions and **b** with over-etch and asymmetries

shown by the corresponding theoretical analysis (Rocha et al. 2004):

$$V_{pr} = V_{pl} = \sqrt{\frac{8}{27}\frac{d_0^3 k}{\varepsilon_0 w l}}. \quad (1)$$

Here d_0 is the capacitor initial gap, k is the mechanical spring constant, $\varepsilon_0 = 8.8546 \times 10^{-12}$ F/m is the air electrical permittivity and w and l are the capacitor plate width and length, respectively.

The fabrication processes used in MEMS are not ideal, and it is often the case that dimension fluctuations are observed. Typical process variations in surface micromachining processes are mainly due to the etching process (over-etching (Clark et al. 2004), scalloping, notching and non-vertical etched walls), material properties (Young's Modulus (E) and density deviations) and deposition (residual stresses and the gradient therein). Since the pull-in voltage value depends on the last-mentioned parameters, pull-in measurements are a suitable and simple approach for estimating technological and other non-idealities and for use as a diagnostic mechanism. Moreover, it can be implemented using simple electronic circuits. This concept was introduced by Rocha et al. (2008) and it was used to identify process-induced variations in the actual device geometry.

2.1 Pull-in based test mechanism

Deep reactive ion etching (DRIE) fabrication steps lead commonly to over-etching of the physical structures compared to the original mask layout. The direct consequence is a reduction in the dimensions of the actual devices compared to the designed ones. Over-etching can be considered uniform at the scale of one microfabricated device (Clark et al. 2004), which means that all layout dimensions will be affected by the same over-etching parameter α (Fig. 1b). This will affect both left and right pull-in voltages. Small gap mismatches (a few nm in misalignment) are also normally observed in fabricated devices. These variations are due to the combined effect of both the deviations introduced by the etching (scalloping, notching and non-vertical etched walls) and the lateral gradient in the stresses and can be modelled as a single gap mismatch (β). Since the gap mismatch affects the left and right pull-in voltages, V_{pl} and V_{pr} differently, these pull-in voltages can be used to estimate β. The estimation of the parameter α is not straightforward, since the pull-in voltage also depends on the Young's Modulus (polysilicon average value is around 160 GPa, but it can show large deviations (Gad-el-Hak 2002)). However, α can be estimated if we introduce a new measurement; the resonance frequency. This does not significantly complicate the approach, since the resonance frequency, although depending on the parameters mentioned, will enable to compute a process based initial model and therefore one single measurement is required.

In order to demonstrate the test mechanism concept, a simple device as the one depicted in Fig. 1a is considered (the main characteristics are shown on the first column of Table 1). The concept relies on the existence of models that take into account the over-etching effect, α, Young's Modulus changes, E, and gap mismatch, β (Table 1). A sequence of steps is performed to extract the three parameters of interest from experimental measurements:

1. Compute the device properties considering layout dimensions and materials average properties (second column on Table 1);
2. Change α until the computed resonance frequency is the same as the measured one: $f_0 = f_r$ (third column on Table 1);
3. Change β and E until the measured pull-in voltages are the same as the computed ones: $V_{pr} = V_{cr}$ and $V_{pl} = V_{cl}$ (forth column on Table 1);
4. Repeat steps 2 and 3 until the three measured values (resonance frequency and left and right pull-in voltages) are the same as the computed ones (last column on Table 1);

Table 1 Example of the test mechanism concept using simulated data

Model		Step 1 $\alpha = 0$ $\beta = 0$ $E = 170$ GPa	Step 2 $\alpha = 209$ nm $\beta = 0$ $E = 170$ GPa	Step 3 $\alpha = 209$ nm $\beta = 25$ nm $E = 162$ GPa	Step 4 $\alpha = 184$ nm $\beta = 25$ nm $E = 160$ GPa
Mechanical domain	$k(\alpha, E) = -\frac{E}{8.8\times10^{4}}\alpha + \frac{E}{170\times10^{9}}$ (N/m)	1 N/m	0.596 N/m	0.568 N/m	0.60 N/m
	$m(\alpha) = -0.75 \times 10^{-3}\ \alpha + 1 \times 10^{-9}$ (Kg)	1 μg	0.84 μg	0.84 μg	0.86 μg
	$f_r(\alpha, E) = \frac{1}{2\pi}\sqrt{\frac{k(\alpha,E)}{m(\alpha)}}$ (Hz)	**5,107 Hz**	**4,205 Hz**	**4,116 Hz**	**4,198 Hz**
Electrical domain	$d_r = 2 \times 10^{-6} + 2\alpha - \beta$ (m)	2 μm	2.418 μm	2.393 μm	2.343 μm
	$d_l = 2 \times 10^{-6} + 2\alpha + \beta$ (m)	2 μm	2.418 μm	2.443 μm	2.393 μm
	$N = 12$ (number of parallel capacitors)	12	12	12	12
	$l = (282 \times 10^{-6} - 2\alpha)\ N$ (m)	3.384 mm	3.379 mm	3.379 mm	3.379 mm
	$w = 10.6 \times 10^{-6}$ (m)	10.6 μm	10.6 μm	10.6 μm	10.6 μm
Pull-in	V_{cr} (α, β, E) (Eq. 1)	**2.770 V**	**2.796 V**	**2.687 V**	**2.682 V**
	V_{cl} (α, β, E) (Eq. 1)	**2.770 V**	**2.796 V**	**2.772 V**	**2.768 V**
Measurements	Right pull-in	$V_{pr} = 2.683$ V			
	Left pull-in	$V_{pl} = 2.770$ V			
	Resonance frequency	$f_0 = 4{,}205$ Hz			

Bold data represent the computed resonance frequency and pull-in voltages

This example, considers a simple geometry and a linear behaviour and therefore Eq. 1 can be used. If the model is more complex, due to the device geometry and any non-linearity in the electro-mechanical behaviour (e.g. fringe fields), the solution of the system of equations, $\partial U_p/\partial x = 0$ and $\partial^2 U_p/\partial x^2 = 0$, cannot be analytically solved and a numerical solution must be used. A possible way to solve for the pull-in voltage in complex models is described by Rocha et al. (2004), where a continuation method tracks the equilibrium points for increasing voltage until the stability is lost. This approach was successfully tested in 2-DOF devices.

One disadvantage of the proposed technique is that it uses device models to predict the electro-mechanical behaviour. As already mentioned, these models can be very complex, and therefore the modelling becomes one of the critical parts of the proposed calibration method. More details about the test mechanism can be found in the work by Rocha et al. (2008), where all the relevant non-idealities, including fringe-fields, are taken into consideration.

3 Auto-calibration method

A MEMS capacitive accelerometer is a second order mechanical system. In the linear approximation, the mechanical structure can be described mathematically as a second order differential equation (considering the existence of an electrostatic actuation mechanism):

$$m\frac{d^2x}{dt^2} + b\frac{dx}{dt} + kx = ma_{ext} + F_{elect}(V), \tag{2}$$

where x is the displacement of the proof mass, a_{ext} is the external acceleration, b is the damping coefficient, k is the mechanical spring constant, m is the proof mass and $F_{elect}(V)$ is the electrostatic force applied to the movable structure for a given voltage V. If the applied voltage is zero, the mechanical system has a resonance frequency given by $\omega_n = \sqrt{\frac{k}{m}}$, while the (DC) sensitivity is $S = \frac{m}{k}$.

For a typical calibration procedure the mechanical spring constant and the mass of the accelerometer are the parameters of interest, while the dynamic behaviour is less important (calibration is mainly performed in static mode, so that only simple electronic circuits are required). As the dynamic behaviour can be neglected in static equilibrium, the balance of forces acting on the accelerometer can be written as:

$$kx = F_{elect}(V) + ma_{ext}. \tag{3}$$

Equation 3 shows that there are two alternative ways to achieve a certain displacement x: by controlling the applied voltage, while maintaining a zero external acceleration or by applying an external acceleration with no voltage applied. The proposed calibration method uses the first option to perform the calibration by estimating the full accelerometer details (using the test method proposed by Rocha et al. (2008)) and applying ±1 g equivalent test signals (using electrostatic forces) to the actuation capacitors to calibrate the full system (device plus readout electronics).

4 Experimental results

Accelerometers fabricated using Bosch epi-poly process (http://www.bosch-sensortec.com accessed 26 June 2010) were used to evaluate the proposed auto-calibration method. A drawing of the device used is shown in Fig. 2.

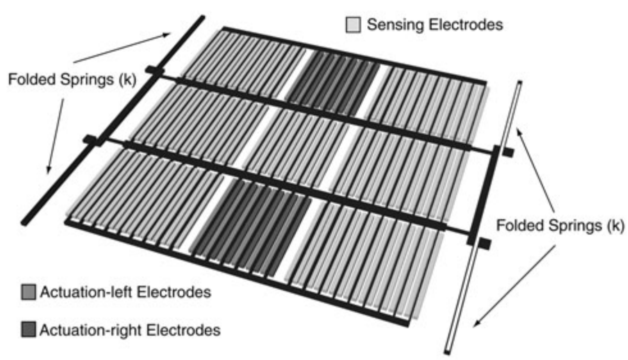

Fig. 2 Illustration of the accelerometer

4.1 Fabricated accelerometers

The fabricated accelerometers (Fig. 3) are composed of four folded springs, 340 μm long and 3 μm wide (layout dimensions), connected to two rigid central bars of about 1 mm long. Parallel-plate capacitors with a 2 μm gap are used for actuation. The displacement measurement involves sensing of the change in capacitance in various sets of differential parallel-plate capacitors, which are also separated by a 2 μm gap. The main device layout parameters and bulk material properties are shown in Table 2.

4.2 Experimental measurements

Experimental measurements were performed on fabricated devices to validate the proposed auto-calibration method. Initially, the pull-in test mechanism was used (Rocha et al. 2008). It should be noted that the model proposed by Rocha et al. (2008) and used in this work takes into account the non-linear behaviour of the device, including fringe-fields. The resonance frequency was determined by acquiring the devices free oscillations (in vacuum) followed by a FFT. The pull-in voltages are obtained from displacement measurements performed during actuation voltage changes (increase of the actuation voltage from zero until an abrupt

Fig. 3 Fabricated accelerometer

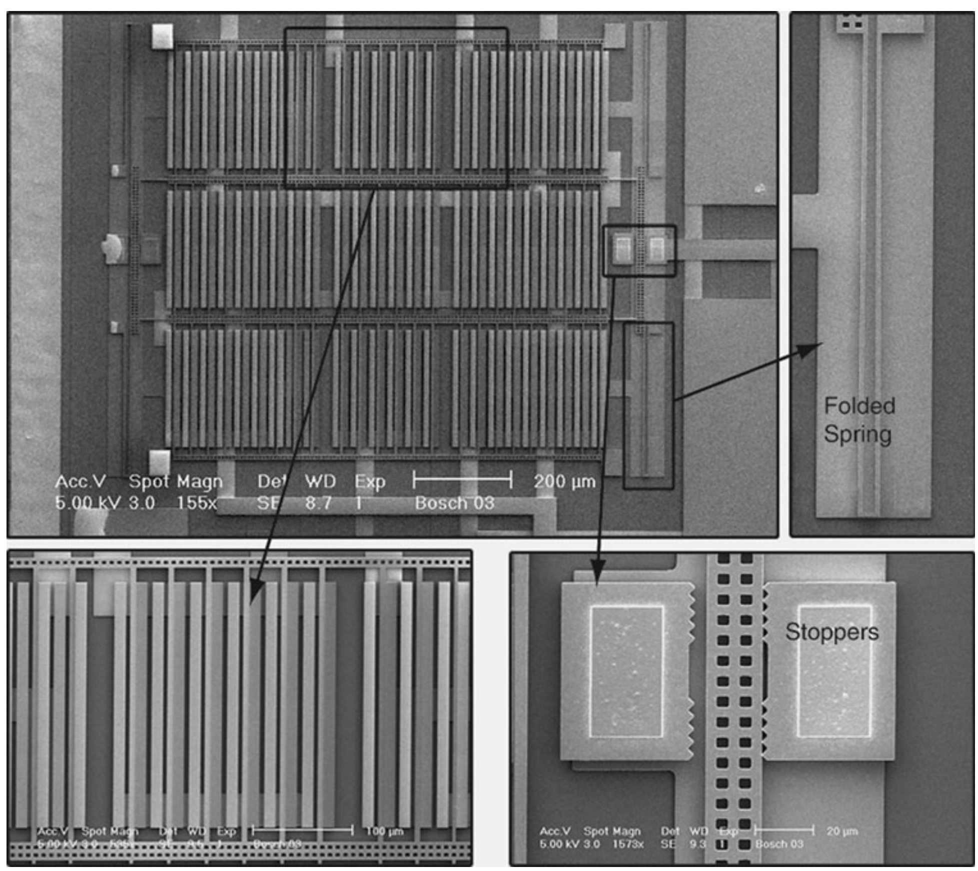

Table 2 Main nominal parameters of the device (layout dimensions and bulk material mean values)

Parameter	Value
Spring length (l)	340 μm
Spring width (b)	3 μm
Mechanical layer thickness (h)	10.6 μm
Spring constant ($k = \frac{2b^3Eh}{l^3}$)	2.38 N/m
Capacitor length (l_c)	282 μm
Capacitor width (w_c)	10.6 μm
Capacitor gap (d_0)	2 μm
No. of actuation capacitors	12
No. of sensing capacitors	52
Young's modulus (E)	163 GPa (Poly-Si)
Density (ρ)	2.5 g cm^{-3}

Table 3 Measurements and estimated accelerometer parameters using the pull-in based test method (Rocha et al. 2008)

	Value
Measurements	
Pull-in voltage left (V_{pl})	3.942 V
Pull-in voltage right (V_{pr})	3.788 V
Resonance frequency	2,740 Hz
Estimated technological parameters	
Over-etching (α)	255 nm
Mismatch (β)	34.5 nm
Young's modulus (E)	147.8 GPa
Estimated accelerometer parameters	
Capacitor gap right ($d_r = d_0 + 2\alpha - \beta$)	2,475.5 nm
Capacitor gap left ($d_l = d_0 + 2\alpha + \beta$)	2,544.5 nm
Mass (m)	3.978 μg
Mechanical spring (k)	1.18 N/m

change is detected). Since the voltage increments can be very small (around 100 μV), it is possible to obtain the pull-in voltage values with a very good accuracy. The voltage at which an abrupt change is detected corresponds to the pull-in voltage. Pull-in measurements also enable the detection of non-functional devices, i.e. non-functional devices show no displacement when actuation voltages are applied and stiction is detected in devices showing full displacement with no voltage applied. The estimated model parameters of one device after measurements are shown in Table 3.

According to the estimated accelerometer parameters, the tested accelerometer has a sensitivity of $S = 3.3702 \times 10^{-9}$ kg/N m. Therefore, a ±1 g will generate a displacement of ±33 nm. Similarly, if one uses the estimated accelerometer model, the voltage necessary to achieve the same displacement of ±33 nm can be computed. Considering that a positive displacement occurs when a voltage is applied to the left-hand electrode and a negative one, for a right-hand electrode actuation, the following voltages levels are found:

$$\begin{aligned} V_{+1g} &= 1.14\,\mathrm{V} \\ V_{-1g} &= 1.11\,\mathrm{V} \end{aligned} \quad (4)$$

After estimation of the necessary voltages to achieve an equivalent ±1 g, two different experiments were made in order to validate the proposed calibration method. First, the response of the accelerometer to a ±1 g external acceleration was recorded. The measured output voltage is shown in Fig. 4.

Subsequently, the accelerometer response to an increasing voltage on the electrodes, in the absence of an external acceleration, was verified. The measured results are presented in Fig. 5.

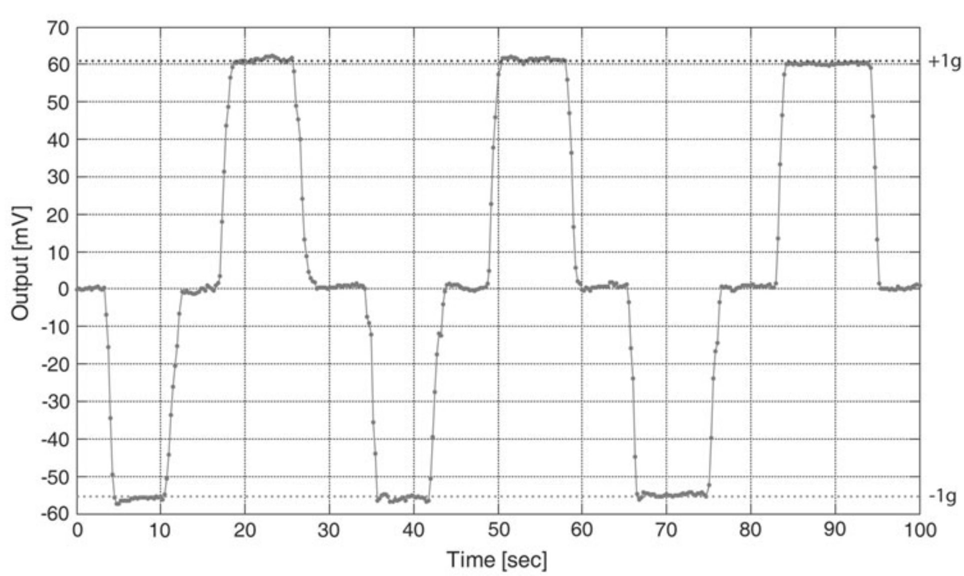

Fig. 4 Response to a ±1 g external acceleration

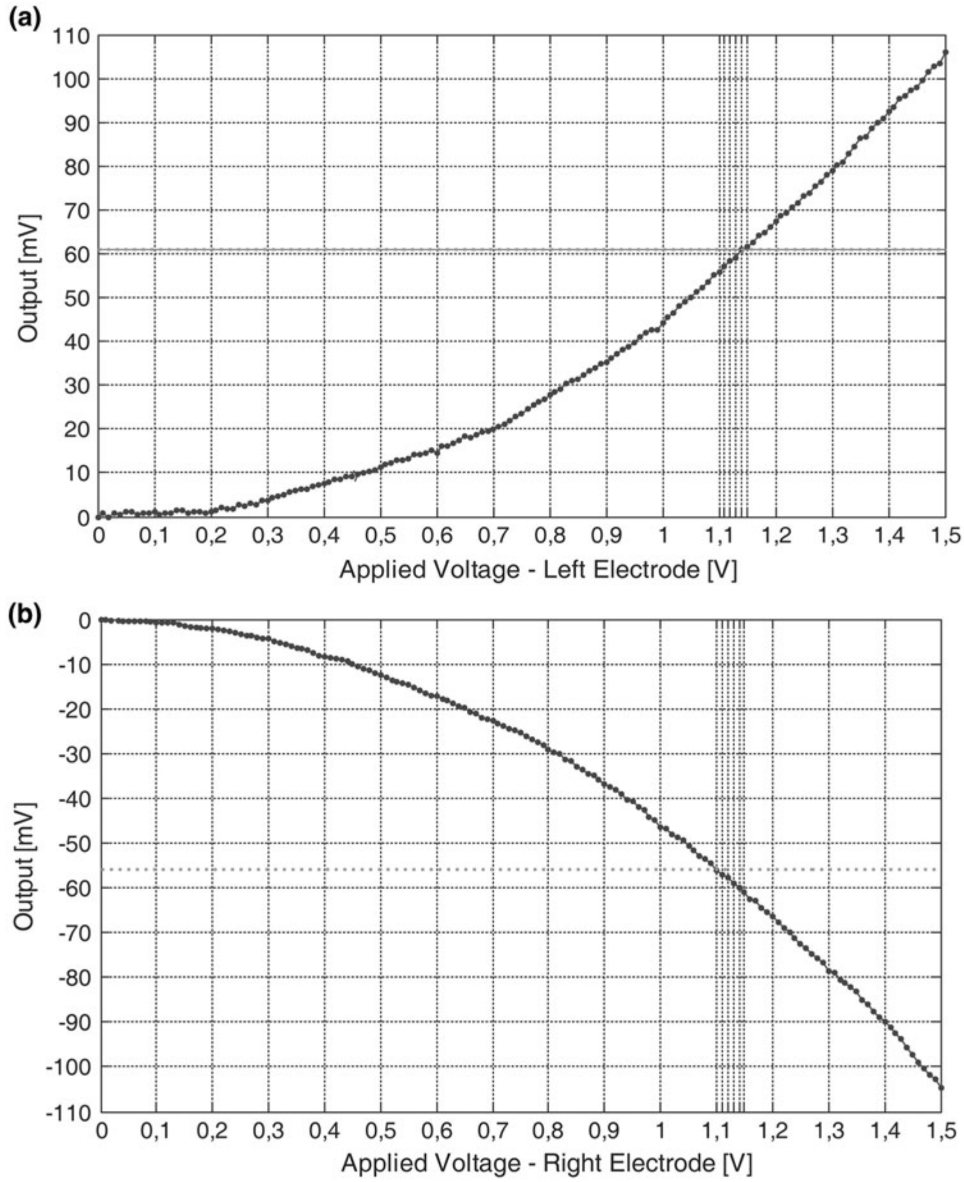

Fig. 5 Response to an applied voltage in **a** *left* electrodes and **b** *right* electrodes

5 Discussion

The measured values presented in Figs. 4 and 5 are very promising and clearly indicate that electric calibration is feasible in capacitive accelerometers. The results demonstrate that the output voltage to +1 g external acceleration is equivalent to the response when a voltage of 1.14 V is applied to the right electrodes (61 mV output voltage), while the response to an actuation voltage of 1.11 V on the left electrodes corresponds to output voltage for an applied external acceleration of −1 g. These results also prove that the estimated model offers a good description of the actual static behaviour of the accelerometer. To further verify model validity, extra measurements were performed: left and right pull-in voltages were measured in the presence of a ±1 g external acceleration and compared with the pull-in voltages given by the models for this situation. Since a ±1 g generates a displacement of ±33 nm, this can be included in the model as a new β (mismatch). Therefore, a +1 g is equivalent to $\beta = 67.5$ nm while a −1 g corresponds to $\beta = 1.5$ nm. The experimental and computed results are shown in Table 4. Once again, the very good agreement between measured and computed values using the estimated model validates the proposed calibration approach.

6 Conclusions

This paper introduces a pull-in based solution for MEMS capacitive accelerometer auto-calibration. The solution was validated through experimental measurements, which

Table 4 Comparative values between measured and estimated pull-in voltages for different external accelerations

		Measured values (V)	Computed values (V)
0 g	Pull-in voltage left	3.942	3.943
	Pull-in voltage right	3.788	3.786
+1 g	Pull-in voltage left	4.019	4.018
	Pull-in voltage right	3.712	3.712
−1 g	Pull-in voltage left	3.867	3.868
	Pull-in voltage right	3.862	3.861

compared favourably with the theoretical non-linear models. Experimental results showed that the response to a ±1 g external acceleration can be replaced by an equivalent asymmetric actuation voltage, allowing a pure electronic calibration of the sensor. The technique can be used in capacitive inertial sensors (e.g. accelerometers and angular rate sensors) and can be extended to full autonomous self-calibrated systems.

While self-testing is already widely used in commercial inertial MEMS, auto-calibration systems, to the author's knowledge, are still inexistent. Calibration during life cycle requires consideration of long-term effects, such as dielectric charging (Rocha et al. 2003; Rottenberg et al. 2007), which results from continuous bias-loading of the accelerometer movable part, stress relaxation and Young's Modulus changes. Since these effects will have an impact on the pull-in voltage, it is always possible through new pull-in voltage measurements to recalculate the parameters of interest (in this case only E and β, since there won't be any changes on the geometry and mass—α is constant). Basically, the pull-in voltages are used to calibrate the model, while the model is used to calibrate the capacitive accelerometer.

Although the results demonstrate the feasibility of auto-calibration in capacitive MEMS, a number of additional provisions must be made if this method is to be applied to in-operation accelerometer calibration. A crucial element for the proposed method is the knowledge of the resonance frequency. This measurement just needs to be performed once, and can be done during the production cycle and stored in a memory registry. Alternatively the measurement of right and left pull-in voltages in the presence of ±1 g allows determining the mass of the device, and therefore the resonance frequency (the spring value is retrieved from pull-in measurements). This alternative way to measure the mass of the device can be very useful when the natural frequency of an overdamped device needs to be known (this is indeed an important outcome of the work presented in this paper—see results of Table 3).

For in-operation pull-in voltage measurement, a variable voltage generator is needed. A possibility is the use of a circuit based on a digital-to-analogue converter (DAC) to generate a ramp and detect the pull-in transition. This option does not add too much circuitry to a normal accelerometer, and if a look-up table is implemented with the necessary calibration voltages (accordingly to the measured pull-in voltages), the full calibration system can be implemented on-chip. Basically, the overall system allows for in-operation testing and auto-calibration.

References

Allen HV, Terry SC, De Bruin DW (1989) Accelerometer systems with self-testable features. Sensors and Actuators A 20:153–161

Analog Devices (2010) Product Datasheets. Norwood, MA. http//:www.analog.com

Charlot B, Mir S, Parrain F, Courtois B (2001) Generation of electrically induced stimuli for MEMS self-test. J Electron Test Theor Appl 17:459–470

Cho ST, Najafi K, Wise KD (1992) Internal stress compensation and scaling in ultra-sensitive silicon pressure sensors. IEEE Trans Electron Devices 39:836–842

Clark JV, Garmire D, Last M, Demmel J, Govindjee S (2004) Practical techniques for measuring MEMS properties. Proc Nanotech 2004:402–405

Gad-el-Hak M (2002) The MEMS Handbook, chap 3. In: Mechanical properties of MEMS materials, CRC Press, USA

Mir S, Rufer L, Dhayni A (2006) Built-in-self-test techniques for MEMS. Microelectron J 37:1591–1597

Olbrich T, Richardson A, Vermeiren W, Straube B (1997) Integrating testability into microsystems. Microsyst Technol 3:72–79

Osterberg PM, Senturia SD (1997) M-TEST: a test chip for MEMS material property measurement using electrostatically actuated test structures. J Microelectromech Syst 6:107–118

Puers R, Reyntjens S (2002) RASTA—real-acceleration-for-self-test accelerometer: a new concept for self-testing accelerometers. Sens Actuators A 97–98:359–368

Rocha LA, Cretu E, Wolffenbuttel RF (2003) Stability of a micromechanical pull-in voltage reference. IEEE Trans Instrum Meas 52:457–460

Rocha LA, Cretu E, Wolffenbuttel RF (2004) Analysis and analytical modeling of static pull-in with application to MEMS-based voltage reference and process monitoring. J Microelectromech Syst 13:342–354

Rocha LA, Mol L, Cretu E, Wolffenbuttel RF, Machado da Silva J (2008) A pull-in based test mechanism for device diagnostic and process characterization. VLSI Design 2008:1–7

Rottenberg X, De Wolf I, Nauwelaers BKJC, De Raedt W, Tilmans HAC (2007) Analytical model of the DC actuation of electrostatic MEMS devices with distributed dielectric charging and nonplanar electrodes. J Microelectromech Syst 16:1243–1253

Senturia SD (2003) Perspective on MEMS past and future: the tortuous pathway from bright ideas to real products. In: Proceedings Tranducers'03 10–15

Wang L-T, Wu C-W, Wen X (2006) VLSI test principles and architectures: design for testability. Morgan Kaufmann, USA

Xiong X, Wu Y-L, Jone W-B (2005) A dual-mode built-in self-test technique for capacitive MEMS devices. IEEE Trans Instrum Meas 54:1739–1750